Preparation and Physical Properties of Melt-Blown Nonwovens of Biodegradable PLA/Acetyl Tributyl Citrate/FePol Copolyester Blends

Li Cui,[1] Chuan-Long Zhu,[2] Ping Zhu,[1] Chi-Hui Tsou,[3] Wen-Jie Yang,[2] Jen-Taut Yeh[1,2,3,4,5]

[1]*Key Laboratory of Green Processing and Functional Textiles of New Textile Materials, Wuhan Textile University, Ministry of Education, Wuhan, China*
[2]*Ministry of Education, Key Laboratory for the Green Preparation and Application of Functional Materials, Faculty of Materials Science and Engineering, Hubei University, Wuhan, China*
[3]*Graduate School of Materials Science and Engineering, National Taiwan University of Science and Technology, Taipei, Taiwan*
[4]*Department of Polymer Materials, Kun Shan University, Tainan, Taiwan*
[5]*School of Printing and Packaging, Wuhan University, Wuhan, China*

Received 15 July 2011; accepted 2 November 2011
DOI 10.1002/app.36429
Published online in Wiley Online Library (wileyonlinelibrary.com).

ABSTRACT: Poly(ethylene glutaric-*co*-terephthalate) copolyester "FePol" (FP) together with a kind of citrate ester plasticizer named acetyl tributyl citrate (ATBC) were chosen to prepare PLA/FP/ATBC blends for melt blowing. Only at 250°C and 10 wt % ATBC content, those $(PLA_xFP_y)_aATBC_b$ specimens are associated with proper rheological properties for processing melt-blown nonwovens. As suggested by SEM, FTIR and DSC analysis, the compatible behavior between PLA and FP molecules was observed as FP content is equal to or less than 5 wt %. Further morphological analysis of $(PLA_xFP_y)_{90}ATBC_{10}$ specimens reveal that relatively fluffy and well-formed nonwoven fabrics were found for $(PLA_xFP_y)_{90}ATBC_{10}$ nonwoven specimens melt-blown at FP contents equal to or lower than 5 wt %. In fact, addition of FP can effectively improve tensile and burst properties of $(PLA_xFP_y)_{90}ATBC_{10}$ nonwovens, wherein their tensile and burst properties approach the maximum values as FP contents reach around 5 wt %. Possible reasons accounting for these melt-blown properties of $(PLA_xFP_y)_{90}ATBC_{10}$ specimens are proposed. © 2012 Wiley Periodicals, Inc. J Appl Polym Sci 000: 000–000, 2012

Key words: poly(lactic acid); melt-blown; nonwoven; rheology; plasticizer

INTRODUCTION

Melt-blown is a one-step process to produce fabrics from thermoplastic polymers. It has become an important industrial technique for its ability of producing fabrics of microfiber structure, which is ideally suited for filtration mediae, thermal insulators, battery separators, oil sorbents, and so on.[1–3] Typical polymers commonly used for melt-blown process are polypropylene (PP), polyethylene, polyethylene terephthalate, polybutylene terephthalate, polytrimethylene terephthalater, polyamide, and polycarbonate.[4–8] Nowadays, over 90% of all melt-blown nonwovens are made from PP because of its low cost, ease of processing, good mechanical properties, little heat shrinkage, chemical inertness, and its ability to be drawn into very fine fibers.[9] Tailor-made PP resins with ultrahigh melt flow rates (MFR) (generally 1000–1500 g/10 min) are most extensively utilized because they have much lower melt viscosities and very narrow molecular weight distributions.[10,11] However, the non-biodegradability of most melt-blown nonwovens has already caused many environmental problems associated with their disposal. Recycling is an environmentally attractive solution but only a minor portion of polymers is recyclable and most end up in municipal burial sites. This leads to the increasingly difficult problem of finding available landfill areas.

Poly(lactic acid) (PLA) is one of the most widely used biodegradable polyesters that can be produced from renewable resource, such as, starch via fermentation processes.[12,13] It is highly accepted as biomedical materials because of its biocompatibility together with relatively well mechanical properties.[14,15]

Correspondence to: J.-T. Yeh (jyeh@mail.ntust.edu.tw).
Contract grant sponsor: Department of Industrial Technology, Ministry of Economic Affairs; contract grant numbers: 95-EC-17-A-11-S1-057, 96-EC-17-A-11-S1-057, 97-EC-17-A-11-S1-057, 99-EC-17-A-11-S1-155.
Contract grant sponsor: National Science Council; contract grant numbers: NSC 95-2221-E-253 -008 -MY3, NSC 99-2221-E-011-010-MY3.

Plenty of studies have been carried out to prepare PLA fibers using varying kinds of spinning processes, including melt,[16,17] dry,[18,19] wet,[20] and electro spinning techniques.[21,22] However, very few investigations[9,23,24] have ever been reported on the preparation of PLA melt-blown nonwovens.

To blow PLA resins at extremely high rates, the melt index (MI) values of PLA needed to be increased to proper values. Addition of plasticizer (e.g. citrate ester[25] and triacetine (TAc)[26,27]) in PLA resins was proven as an effective way to increase the MI and processability of PLA resins. In comparison with citrate ester, the thermal stability of TAc is relatively poor and liable to degrade during the melt-blown processes of PLA. Moreover, PLA resins are prone to hydrolysis or degrade at relatively high temperatures during their melt-blown processes. They are also well known for their low tearing resistance and brittle characteristics, especially for melt-blown nonwovens encountered with hydrolysis or thermal degradation. Addition of toughening agents in PLA resins was proven as an efficient way to improve their toughness.[28,29] Among these toughening agents, poly(butylene adipate-*co*-terephthalate) (PBAT) has attracted many attentions because of their highly compatibility with PLA and good processability even after melt-blending with PLA resins.[28] In fact, many commercial biodegradable films were prepared by melt-blending of proper amounts of PBAT in PLA before film-blowing of the PLA/PBAT resins.

Our early investigation[28] found that the values of elongation at break of PLA/poly(butylene adipate-*co*-terephthalate) (PBAT) blends did improve significantly after addition proper amounts of the PBAT in PLA resins. However, the melting temperature of PBAT is significantly lower than that of PLA that can lead to poor compatibility or even phase separation between PLA and PBAT phases during the melt crystallization processes of PLA/PBAT blends. In fact, demarcated PBAT droplets were found dispersed in PLA matrices that often lead to poor tearing resistance and toughness of the PLA/PBAT blends.[28] In comparison with PBAT, our latest research[29] used biodegradable poly(ethylene glutaric-*co*-terephthalate) copolyester "FePol" (FP) with relatively higher melting temperature as the toughening agent for PLA. Somewhat interestingly, the tear resistance values of PLA/FP blown films improved significantly after addition of proper amounts of FP resins, in which the tear resistance values of PLA/FP blown films are significantly better than those of the PLA/PBAT blown films with the same amounts of toughening agent. As far as we know, no investigation has ever been reported on the preparation of PLA melt-blown nonwoven using FP as toughening agent.

In this study, FP together with a kind of citrate ester plasticizer named acetyl tributyl citrate (ATBC) was chosen to prepare PLA/FP/ATBC blends for melt blowing. The influences of the compositions of ATBC and FP on the morphology, rheological and tensile properties of PLA/FP/ATBC nonwovens are reported.

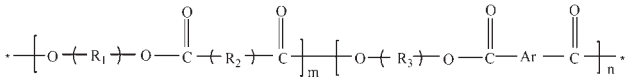

Figure 1 Chemical structure of FP copolyester.

EXPERIMENTAL

Materials and sample preparation

The poly(lactic acid) (PLA) resin used in this study was obtained from Cargill-Dow, with a trade name of Nature green 3051D. Synthetic biodegradable poly(ethylene glutaric-*co*-terephthalate) copolyester "FP" (Melting temperature (T_m) 144°C, thermal degradation temperature (T_d) 296°C, specific gravity 1.24 and melt flow indexes 40 g/10 min at 190°C was purchased from Far Eastern Textile with a trade name of FP2040, which was used as the compatibilizer to blend with PLA for better preparation of the melt-blown nonwovens. The chemical structure of the FP copolyester is shown in Figure 1. Analytical grade acetyl triethyl citrate (ATBC) was used as plasticizer in this study, which was kindly supplied by Yixing Chemical Company, Jiangsu, China. Before melt-blending, PLA and FP resins were dried to a moisture content of 250 ppm in a dehumidifier drier at 80°C for 4 h. Varying compositions of dried components of PLA, FP together with ATBC were melt-blended using a Jiant SHJ-20 twin-screw extruder, which was purchased from Giant Machiney Corporation, Nanjing, China. During each compounding process, the extruder was operated at 140°C in the feeding zone and at 170°C towards the extrusion die with a screw speed of 120 rpm. The $(PLA_xFP_y)_aATBC_b$ blends obtained from the twin screw extruder were quenched in cold water at 15°C and cut into the pellet form. The compositions of the $(PLA_xFP_y)_aATBC_b$ resins prepared in this study are summarized in Table I.

Preparation of melt-blown nonwovens

Before melt-blowing, the $(PLA_xFP_y)_aATBC_b$ resins were dried to a moisture content of 250 ppm in a hehumidifier drier at 80°C for 4 h. The dehumidifier dried $(PLA_xFP_y)_aATBC_b$ resins were then melt-blown using a Huada melt-blowing machine model F-6D, which was manufactured by Yantai Huada Masterbatch & Machinery Corporation, Yantai, China. During each melt-blown experiment, the melt-blown machine was operated at 210°C in the

TABLE I
Compositions of $(PLA_xFP_y)_aATBC_b$ Specimens

Samples	PLA (wt %)	FP (wt %)	ATBC (wt %)
PLA_{100}	100	0	0
$PLA_{97.5}FP_{2.5}$	97.5	2.5	0
$PLA_{95}FP_5$	95	5	0
$PLA_{92.5}FP_{7.5}$	92.5	7.5	0
$PLA_{90}FP_{10}$	90	10	0
$PLA_{85}FP_{15}$	85	15	0
$PLA_{80}FP_{20}$	80	20	0
$PLA_{95}ATBC_5$	95	0	5
$(PLA_{97.5}FP_{2.5})_{95}ATBC_5$	92.63	2.37	5
$(PLA_{95}FP_5)_{95}ATBC_5$	90.25	4.75	5
$(PLA_{92.5}FP_{7.5})_{95}ATBC_5$	87.88	7.12	5
$(PLA_{90}FP_{10})_{95}ATBC_5$	85.50	9.50	5
$(PLA_{85}FP_{15})_{95}ATBC_5$	80.75	14.25	5
$(PLA_{80}FP_{20})_{95}ATBC_5$	76.00	19.00	5
$PLA_{90}ATBC_{10}$	90	0	10
$(PLA_{97.5}FP_{2.5})_{90}ATBC_{10}$	87.75	2.25	10
$(PLA_{95}FP_5)_{90}ATBC_{10}$	85.50	4.50	10
$(PLA_{92.5}FP_{7.5})_{90}ATBC_{10}$	83.25	6.75	10
$(PLA_{90}FP_{10})_{90}ATBC_{10}$	81.00	9.00	10
$(PLA_{85}FP_{15})_{90}ATBC_{10}$	76.50	13.50	10
$(PLA_{80}FP_{20})_{90}ATBC_{10}$	72.00	18.00	10
$PLA_{85}ATBC_{15}$	85	0	15
$(PLA_{97.5}FP_{2.5})_{85}ATBC_{15}$	82.88	2.12	15
$(PLA_{95}FP_5)_{85}ATBC_{15}$	80.75	4.25	15
$(PLA_{92.5}FP_{7.5})_{85}ATBC_{15}$	78.63	6.37	15
$(PLA_{90}FP_{10})_{85}ATBC_{15}$	76.50	8.5	15
$(PLA_{85}FP_{15})_{85}ATBC_{15}$	72.25	12.75	15
$(PLA_{80}FP_{20})_{85}ATBC_{15}$	68.00	17	15

feeding zone, 250°C towards the spinneret and at a screw speed of 100 rpm. A 50-hole die with a distance 1 mm between each orifice center was used in this research. The orifice diameter of each hole was 0.2 mm. The mass flow rate of polymer melt was 0.6 g/min through each die. An air-gap distance of 1 mm was employed, which supplies 350°C heated air with an air flow rate around 260 m/s. The perpendicular distances from the spinneret to the conveyer varied from 300 to 700 mm for the $(PLA_xFP_y)_aATBC_b$ resins prepared above. To prepare melt-blown nonwovens with different thickness, the conveyor was operated at a rate ranging from 6 to 12 m/min. The prepared nonwovens are classified as thin, medium and thick nonwoven specimens, when they were prepared using a conveying rate of 12, 8, and 6 m/min, respectively.

Melt index analysis

The melt index (MI) values of the $(PLA_xFP_y)_aATBC_b$ resins were measured using a Gotech Melt Indexer GT-MI7100 equipped with a load of 2.16 kg at various temperatures. Before testing, $(PLA_xFP_y)_aATBC_b$ resins were vacuum dried at 80°C for 4 h. The MI values of $(PLA_xFP_y)_aATBC_b$ were measured at 190, 210, 230, 240, 250, 260, and 270°C, respectively.

Rheological and melt strength properties

The melt shear viscosities (η_s) of the PLA and $(PLA_xFP_y)_{90}ATBC_{10}$ blends were measured at 190°C and shear rates ranging from 500 to 5000 s^{-1} using a Gotech Rheotester CR-6000 Capillary Rheometer equipped with a capillary of 1 mm diameter. Before testing, PLA and $(PLA_xFP_y)_{90}ATBC_{10}$ resins were vacuum dried at 80°C for 4 h. These η_s measured at various shear rates up to about 5000 s^{-1} are used to correlate with the melt-blown behavior of $(PLA_xFP_y)_{90}ATBC_{10}$ resins, because the shear rates of polymer melts during melt-blowing are generally recognized to be less than several thousand s^{-1}.

The melting volumetric flow rate through the capillary is given as:

$$Q = \frac{\pi R^3}{4}\gamma\frac{4n}{3n+1}, \quad (1)$$

where R is capillary radius, r is shear rate at the capillary wall, and n is flow index depending on the temperature. The term $\frac{4n}{3n+1}$ is the Rabinowitsch correction factor.

Pressures are monitored, and shear stress values are calculated by the following equation:

$$\tau = \frac{\Delta PR}{2L}, \quad (2)$$

where ΔP is the pressure at the capillary entrance, R and L are radius and length of the die (mm), respectively.

According to Onteniente,[30] if a thermoplastic material obeys power-law behavior:

$$\tau = K\gamma^n \quad (3)$$

The apparent viscosity η is defined by eq. (4):

$$\eta = \tau/\gamma \quad (4)$$

where τ is shear stress; γ is shear rate at the capillary wall; K is consistency of the materials depending on the temperature, the structure and the formulation of the polymer.

Melt strength values of $(PLA_xFP_y)_aATBC_b$ resins were performed on CEAST Rheologic 5000 capillary rheometer at 170°C. The melt strength values were used to correlate with the uniaxial extensional performance of polymer melts during the melt-blown processes.

Fourier transform infrared spectroscopy

The PLA, FP, and $(PLA_xFP_y)_aATBC_b$ specimens used for Fourier transform infrared (FTIR) spectroscopic analysis were prepared by hot-pressing small

amounts (ca., 5.0 mg) of the vacuum dried PLA, FP, and melt-blended $(PLA_xFP_y)_aATBC_b$ resins at 190°C and 10 MPa for 2 min and then cooled in air at 25°C. The thickness of the hot-pressed films were prepared sufficiently thin (ca., 0.02 mm) enough to obey the Beer-Lambert law. Fourier transform infrared spectroscopic measurements of $(PLA_xFP_y)_aATBC_b$ specimens were recorded on a Nicolet Avatar 320 FTIR spectrophotometer at 25°C, wherein 32 scans with a spectral resolution 1 cm^{-1} were collected during each spectroscopic measurement.

Thermal properties

Thermal properties of $(PLA_xFP_y)_aATBC_b$ resins were determined using a TA Q100 differential scanning calorimetry (DSC) instrument. All DSC scans were carried out at a heating rate of 40°C/min and under flowing nitrogen at a flow rate of 50 mL/min. The instrument was calibrated using the pure indium. Samples weighing about 15 and 0.5 mg were placed in standard aluminum sample pans for glass transition (T_g) and melting (T_m) temperatures determination of each specimen, respectively.

Morphology analysis

The original and fracture surface morphology of $(PLA_xFP_y)_aATBC_b$ nonwoven samples were examined using a Joel JSM-5200 Scanning Electron Microscopy (SEM). The $(PLA_xFP_y)_aATBC_b$ nonwoven specimens were gold-coated at 15 kV for 15 s before SEM examinations.

Weights and thicknesses of melt-blown nonwovens

The weights of $(PLA_xFP_y)_aATBC_b$ melt-blown nonwoven specimens were measured according to ISO 9862 standard. The rectangular $(PLA_xFP_y)_aATBC_b$ nonwoven specimens with a dimension of 100 × 100 mm^2 were sectioned from the melt-blown nonwovens prepared in the "Preparation of Melt-blown Nonwovens" section. The thicknesses of $(PLA_xFP_y)_aATBC_b$ nonwoven specimens were measured with an applied pressure of 0.5 KPa according to ISO 9073-2-1989 standard using a YG141 fabric thickness gauge, which was purchased from Wuhan Guoliang Instrument Corporation, Wuhan, China. The weights and thicknesses of each $(PLA_xFP_y)_aATBC_b$ nonwoven specimens were obtained based on the average values of at least five specimens.

Tensile strengths

The rectangular $(PLA_xFP_y)_{90}ATBC_{10}$ nonwoven specimens with a dimension of 200 × 50 mm^2 were prepared from the melt-blown nonwoven specimens according to ISO 9073-3-1989 standard. The tensile strengths of the $(PLA_xFP_y)_{90}ATBC_{10}$ melt-blown specimens were conducted with a crosshead speed of 100 mm/min and a pretension of 5 N using an intelligent electronic tensile testing machine model YG (B) 026-025, which was purchased from Wenzhou Darong Textile Instrument Corporation, Wenzhou, China. The tensile strength values of the nonwoven specimens were obtained based on the average tensile strengths of at least five specimens.

Burst strengths

Circular $(PLA_xFP_y)_{90}ATBC_{10}$ melt-blown nonwoven specimens with a diameter of 25 mm used for burst strength measurements were prepared according to ISO 2960 standard. The burst strengths of $(PLA_xFP_y)_aATBC_b$ melt-blown nonwoven specimens were determined using an intelligent electronic bursting testing machine model YG065H, which was purchased from Laizhou Electron Instrument Corporation, Laizhou, China. A steel ball with a speed of 100 mm/min was used in the burst strength measurements. The burst strength values of the nonwoven specimens were obtained based on the average burst strengths of at least five specimens.

RESULTS AND DISCUSSION

Rheological and melt-blown properties

The melt index (MI) values of $(PLA_xFP_y)_aATBC_b$ specimens measured at various testing temperatures are summarized in Figure 2. As expected, MI values of $(PLA_xFP_y)_aATBC_b$ specimens increase gradually as the testing temperatures raise from 190 to 230°C. In contrast, the MI values of each $(PLA_xFP_y)_aATBC_b$ specimen increase dramatically as the temperatures increase from 230 to 270°C. For instance, MI values of $(PLA_{97.5}FP_{2.5})_{90}ATBC_{10}$ specimens increase dramatically from 340 to 862 and 1430 g/10 min, as the testing temperature raise from 230 to 250 and 270°C, respectively. On the other hand, the MI values of $(PLA_xFP_y)_aATBC_b$ specimens increase significantly with the increase in ATBC contents. In contrast, at a fixed ATBC content, MI values of $(PLA_xFP_y)_aATBC_b$ specimens increase only slightly as the FP contents increase. For instance, the MI value of $(PLA_{85}FP_{15})_{85}ATBC_{15}$ at 250°C reaches 1760 g/10 min, which is significantly higher than that of $(PLA_{85}FP_{15})_{95}ATBC_5$ specimen (1760 vs. 60 g/10 min), but only slightly higher than that of $(PLA_{95}FP_5)_{95}ATBC_{15}$ specimen (1760 vs. 1120 g/10 min).

Only $(PLA_xFP_y)_aATBC_b$ specimens with properly high MI values are suitable for melt-blown processing. As shown in Figure 2, only those

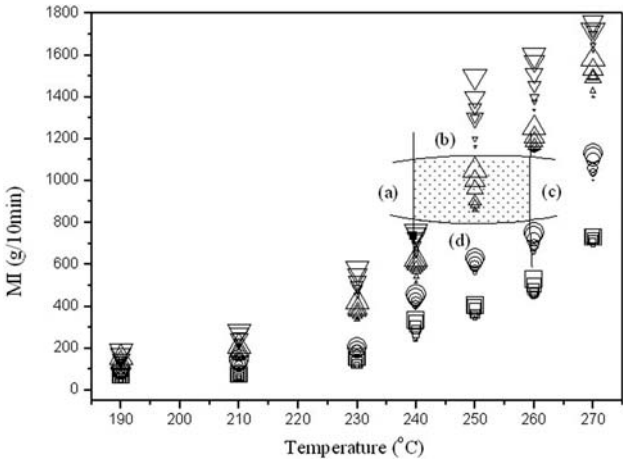

Figure 2 MI values of PLA (□), $PLA_{97.5}FP_{2.5}$ (□), $PLA_{95}FP_5$ (□), $PLA_{92.5}FP_{7.5}$ (□), $PLA_{90}FP_{10}$ (□), $PLA_{85}FP_{15}$ (□), $PLA_{80}FP_{20}$ (□), $PLA_{95}ATBC_5$ (○), $(PLA_{97.5}FP_{2.5})_{95}ATBC_5$ (○), $(PLA_{95}FP_5)_{95}ATBC_5$ (○), $(PLA_{92.5}FP_{7.5})_{95}ATBC_5$ (○), $(PLA_{90}FP_{10})_{95}ATBC_5$ (○), $(PLA_{85}FP_{15})_{95}ATBC_5$ (○), $(PLA_{80}FP_{20})_{95}ATBC_5$ (○), $PLA_{90}ATBC_{10}$ (△), $(PLA_{97.5}FP_{2.5})_{90}ATBC_{10}$ (△), $(PLA_{95}FP_5)_{90}ATBC_{10}$ (△), $(PLA_{92.5}FP_{7.5})_{90}ATBC_{10}$ (△), $(PLA_{90}FP_{10})_{90}ATBC_{10}$ (△), $(PLA_{85}FP_{15})_{90}ATBC_{10}$ (△), $(PLA_{80}FP_{20})_{90}ATBC_{10}$ (△), $PLA_{85}ATBC_{15}$ (▽), $(PLA_{97.5}FP_{2.5})_{85}ATBC_{15}$ (▽), $(PLA_{95}FP_5)_{85}ATBC_{15}$ (▽), $(PLA_{92.5}FP_{7.5})_{85}ATBC_{15}$ (▽), $(PLA_{90}FP_{10})_{85}ATBC_{15}$ (▽), $(PLA_{85}FP_{15})_{85}ATBC_{15}$ (▽) and $(PLA_{80}FP_{20})_{85}ATBC_{15}$ (▽) specimens measured at varying temperatures.

$(PLA_xFP_y)_aATBC_b$ specimens in the shadowed region are associated with proper rheological properties for processing melt-blown nonwovens. At temperatures lower than 240°C and/or ATBC contents less than 10 wt %, the MI values of all $(PLA_xFP_y)_aATBC_b$ specimens are too low to blow melt-blown nonwovens stably, respectively, that often lead to poorly drawn melt-blown fibers and nonwovens during their melt-blown processes [see Fig. 2(a,d)]. As shown in Figure 2(b), at temperatures higher than 240°C and ATBC contents more than 10 wt %, MI values of $(PLA_xFP_y)_aATBC_b$ resins are too high to yield enough melt strengths, and hence, result in melt fracture of melt-blown fibers and poorly formed melt-blown nonwovens during their melt-blown processes. At temperatures higher than 260°C, the poorly formed nonwovens are brown and brittle because $(PLA_xFP_y)_aATBC_b$ resins degrade significantly during their melt-blown processes [see Fig. 2(c)]. Outside of the shadowed region of Figure 2, the temperatures and compositions are not suitable for melt-blowing $(PLA_xFP_y)_aATBC_b$ resins in a stable manner, and are defined as the "un-melt-blown" region.

Fourier transform infrared spectroscopy

Figure 3 illustrates the typical Fourier Transform Infrared (FTIR) spectra of PLA, $PLA_{90}ATBC_{10}$, FP, and $(PLA_xFP_y)_{90}ATBC_{10}$ specimens. Four distinguished absorption bands centered at 1750, 2945, 2995, and 3510 cm^{-1} corresponding to the motions of C=O bending, C—H aliphatic stretching (doublet) and O—H stretching vibrations were found in the spectrum of PLA specimen, respectively. After addition of ATBC plasticizer in PLA, the FTIR spectrum of $PLA_{90}ATBC_{10}$ specimen remains nearly the same as that of the PLA specimen. The FTIR spectrum of FP exhibits three distinguished absorption bands centered at 1730, 2960, and 3308 cm^{-1}, which are attributed to the motions of C=O bending, C—H stretching and O—H stretching vibrations of FP molecules, respectively. The FTIR spectra of $(PLA_xFP_y)_{90}ATBC_{10}$ specimens are similar to that of PLA, wherein the three main absorption bands centered at 2945, 2995, and 3510 cm^{-1} were also found in the spectra of $(PLA_xFP_y)_{90}ATBC_{10}$ specimens. However, the above mentioned 1750 cm^{-1} absorption band originally shown on the FTIR spectra of PLA specimen was gradually replaced by a newly developed absorption band centered at 1770 cm^{-1}, which is suggested corresponding to the motion of ester carbonyl (polyester C=O) stretching vibration.[31] Presumably, the disappearance of the 1750 cm^{-1} C=O bending absorption band and appearance of 1770 cm^{-1} (polyester C=O) stretching absorption band is attributed to the reaction of the carboxylic acid groups of PLA molecules with the hydroxyl groups of FP molecules during the melt-blending of PLA_xFP_y specimens.[29]

Morphology analysis

Typical SEM micrographs of the fracture surfaces of $(PLA_xFP_y)_{90}ATBC_{10}$ specimens are shown in Figure 4. After blending FP in $PLA_{90}ATBC_{10}$ resins, many

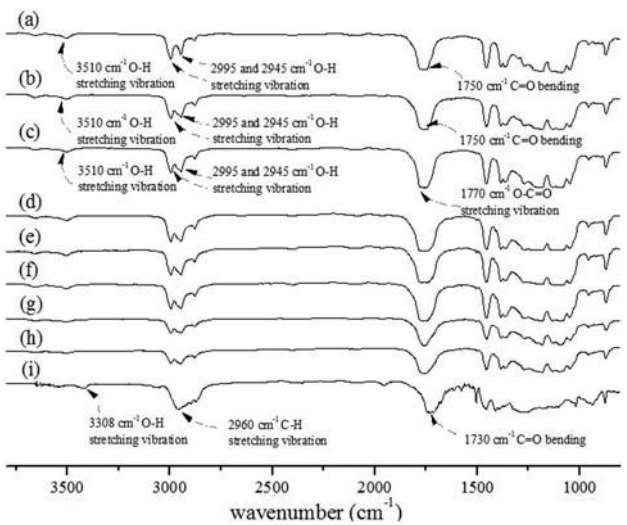

Figure 3 FTIR spectra of (a) PLA, (b) $PLA_{90}ATBC_{10}$, (c) $(PLA_{97.5}FP_{2.5})_{90}ATBC_{10}$, (d) $(PLA_{95}FP_5)_{90}ATBC_{10}$, (e) $(PLA_{92.5}FP_{7.5})_{90}ATBC_{10}$, (f) $(PLA_{90}FP_{10})_{90}ATBC_{10}$, (g) $(PLA_{85}FP_{15})_{90}ATBC_{10}$, (h) $(PLA_{80}FP_{20})_{90}ATBC_{10}$ and (i) FP specimens.

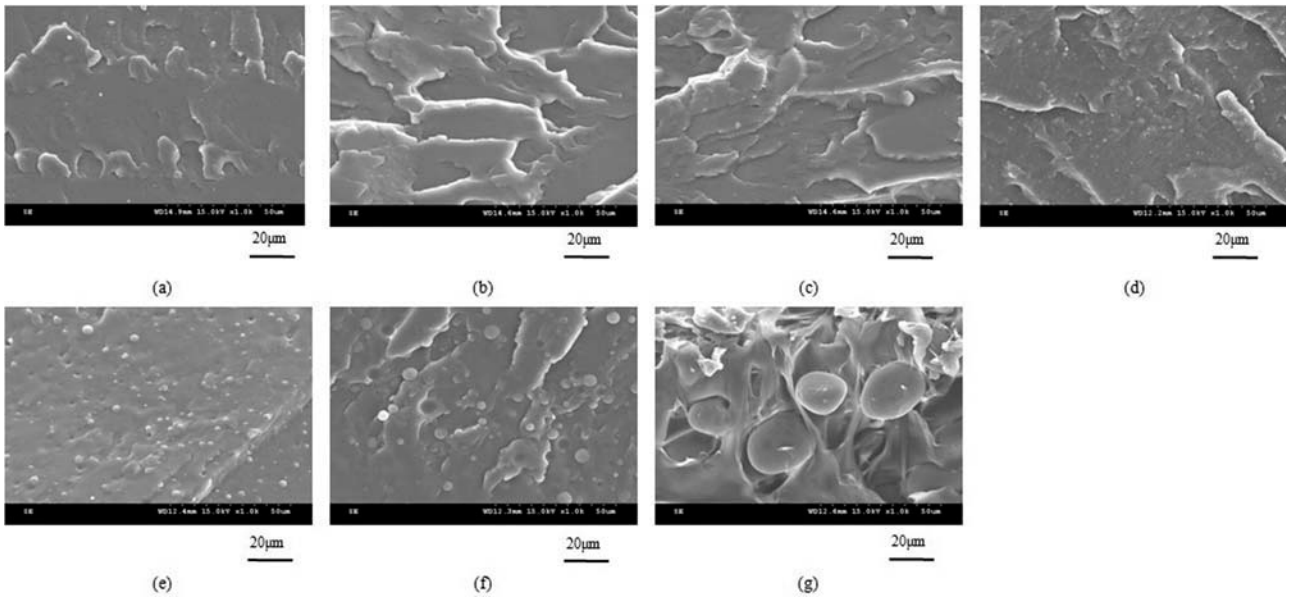

Figure 4 SEM micrographs of the fracture surfaces of (a) $PLA_{90}ATBC_{10}$, (b) $(PLA_{97.5}FP_{2.5})_{90}ATBC_{10}$, (c) $(PLA_{95}FP_5)_{90}ATBC_{10}$, (d) $(PLA_{92.5}FP_{7.5})_{90}ATBC_{10}$, (e) $(PLA_{90}FP_{10})_{90}ATBC_{10}$, (f) $(PLA_{85}FP_{15})_{90}ATBC_{10}$, (g) $(PLA_{80}FP_{20})_{90}ATBC_{10}$ melt-blown nonwovens.

FP droplets were found dispersing in the PLA matrix of the $PLA_{90}ATBC_{10}$ specimens, as their FP contents are more than 5 wt % [see Fig. 4(e–g)]. In fact, the sizes of dispersed FP droplets reduce significantly with decreasing the FP contents. At FP content equal to 5 wt %, a relatively uniform texture without visibly dispersed FP phases was found on the fracture surface of the $(PLA_{95}FP_5)_{90}ATBC_{10}$ specimen. However, as FP contents equal to or less than 5 wt %, the FP molecules appear to be morphologically compatible with PLA molecules without clearly phase-separated FP phases. The distinguished FP droplets dispersing in $(PLA_xFP_y)_{90}ATBC_{10}$ specimens are mainly attributed to the incompatibility between PLA and FP at FP contents more than 5 wt %. These phase-separated FP droplets become more distinguished as the difference in η_s values between FP_xATBC_y and PLA_xATBC_y increases.

Typical SEM micrographs of the surfaces of $(PLA_xFP_y)_{90}ATBC_{10}$ nonwoven specimens are shown in Figure 5. Regardless of the FP contents, diameters of melt-blown fibers in $(PLA_xFP_y)_{90}ATBC_{10}$

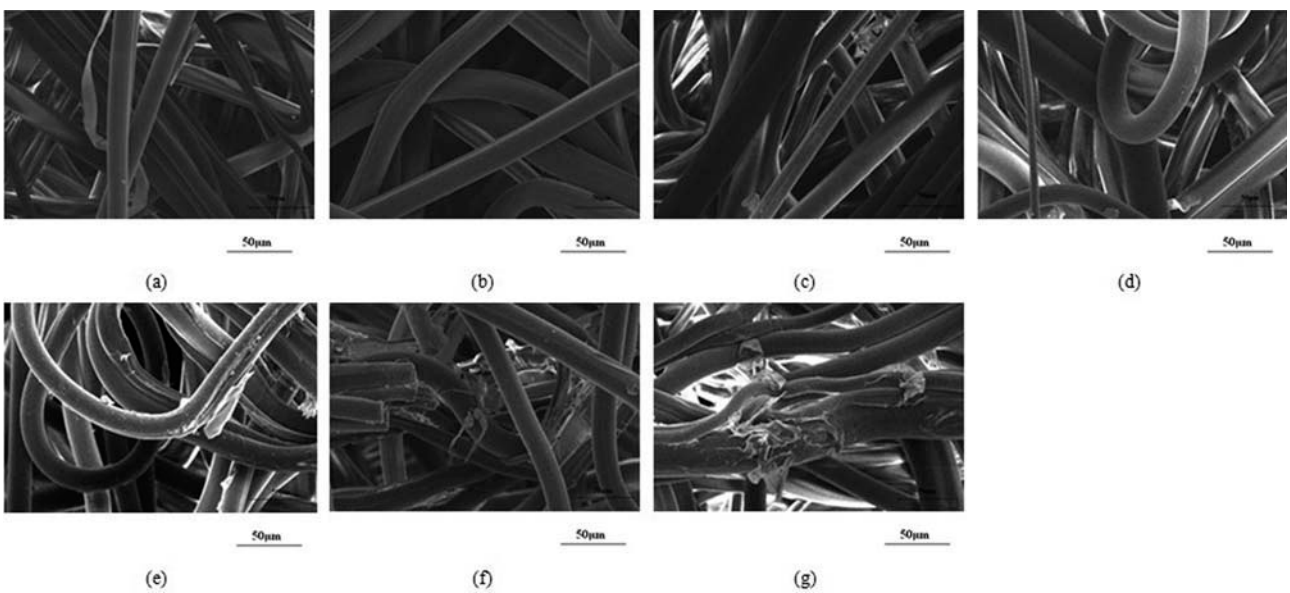

Figure 5 SEM micrographs of the surfaces of (a) $PLA_{90}ATBC_{10}$, (b) $(PLA_{97.5}FP_{2.5})_{90}ATBC_{10}$, (c) $(PLA_{95}FP_5)_{90}ATBC_{10}$, (d) $(PLA_{92.5}FP_{7.5})_{90}ATBC_{10}$, (e) $(PLA_{90}FP_{10})_{90}ATBC_{10}$, (f) $(PLA_{85}FP_{15})_{90}ATBC_{10}$, (g) $(PLA_{80}FP_{20})_{90}ATBC_{10}$ melt-blown nonwovens.

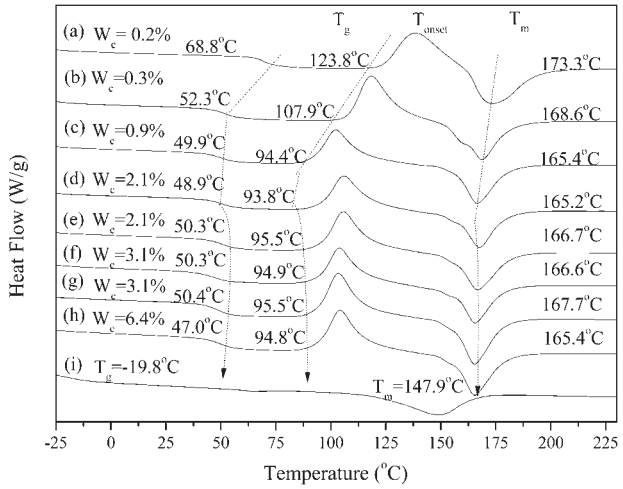

Figure 6 DSC thermograms of (a) PLA, (b) $PLA_{90}ATBC_{10}$, (c) $(PLA_{97.5}FP_{2.5})_{90}ATBC_{10}$, (d) $(PLA_{95}FP_5)_{90}ATBC_{10}$, (e) $(PLA_{92.5}FP_{7.5})_{90}ATBC_{10}$, (f) $(PLA_{90}FP_{10})_{90}ATBC_{10}$, (g) $(PLA_{85}FP_{15})_{90}ATBC_{10}$, (h) $(PLA_{80}FP_{20})_{90}ATBC_{10}$ and (i) FP specimens scanned at 40°C /min.

nonwoven specimens are roughly the same ranging from 10 to 25 μm. Relatively fluffy and well formed nonwoven fabrics were found for $(PLA_xFP_y)_{90}ATBC_{10}$ nonwoven specimens melt-blown at FP contents equal to or lower than 5 wt % [see Fig. 5(a–c)]. Poor melt-blown characteristics with broken filaments gradually appear on $(PLA_xFP_y)_{90}ATBC_{10}$ nonwoven specimens as their FP contents increase [see Fig. 5(e–g)].

Thermal properties

Typical DSC thermograms of PLA, $PLA_{90}ATBC_{10}$, FP, and $(PLA_xFP_y)_{90}ATBC_{10}$ specimens scanned at 40°C/min are summarized in Figure 6. As shown in Figure 6, a thermal transition at temperatures near 68.8°C was observed in the DSC thermogram of PLA specimen, which is generally recognized as the glass transition temperature (T_g) of PLA resins. In addition to the glass temperature transition, a melting endotherm with a peak temperature (T_m) at around 173.3°C was found on the thermogram of PLA specimen. After blending ATBC in PLA resins, the T_g, onset temperatures of recrystallization exotherm (T_{onset}) and T_m values of PLA molecules reduce significantly from 68.8, 128, and 173.3°C to 52.3, 107.9, and 168.6°C, respectively, as the ATBC contents in PLA_xATBC_y specimens increase from 0 to 10 wt %. The reduction of T_g, T_{onset}, and T_m is most likely attributed to the significant increase in the free volume and molecular mobility of the PLA molecules after addition of ATBC plasticizer in PLA resin, since PLA molecules with higher mobility can then recrystallize at lower temperatures and hence, results in crystals with lower melting temperatures.

In contrast to PLA, as shown in Figure 6(i), a much lower thermal transition near −19.8°C was found on the DSC thermogram of FP specimen, which is attributed to the glass transition motion of FP molecules.[29] A board melting endotherm with a peak temperature at around 147.9°C was found on the DSC thermogram of FP specimen. After addition of FP in $PLA_{90}ATBC_{10}$ resin, the T_g, T_{onset}, and T_m values of $(PLA_xFP_y)_{90}ATBC_{10}$ specimens reduce from 52.3, 107.9, and 168.6°C to 48.9, 93.8, and 165.2°C, respectively, as FP contents in $(PLA_xFP_y)_{90}ATBC_{10}$ specimens increase from 0 to 5 wt %. Conversely, the T_g, T_{onset}, and T_m values of $(PLA_xFP_y)_{90}ATBC_{10}$ specimens increase from 48.9, 93.8, and 165.2°C to 50.4, 95.5, and 167.7°C as the FP contents in $(PLA_xFP_y)_{90}ATBC_{10}$ specimens increase from 5 to 15 wt %. As discussed in morphological analysis, FP molecules appear to be compatible with PLA molecules without clearly phase-separated FP phases, when FP contents are equal to or less than 5 wt %. However, at FP contents higher than 5 wt %, distinct FP droplets were found phase-separating from PLA matrices. Presumably, the significant reduction in T_g, T_{onset}, and T_m values of $(PLA_xFP_y)_{90}ATBC_{10}$ specimens with the initial increase in FP contents is attributed to the compatible behavior between PLA and FP molecules, since FP molecules with much lower T_g values can somewhat reduce the T_g values of PLA-rich phases at FP contents less than 5 wt %. On the contrary, the increase in T_g, T_{onset}, and T_m values of $(PLA_xFP_y)_{90}ATBC_{10}$ specimens with further increasing FP contents is ascribed to the occurrence of phase-separated behavior between PLA and FP molecules at FP contents higher than 5 wt %, wherein the excess amounts of FP molecules not only invert but also bring additional FP molecules originally present in the PLA-rich phases into phase-separated FP droplets.

Rheological and melt strength properties

Figure 7 exhibits the melt shear viscosities (η_s) of the PLA and $(PLA_xFP_y)_{90}ATBC_{10}$ resins measured at 190°C and varying shear rates, in which $(PLA_xFP_y)_{90}ATBC_{10}$ resins were proven suitable for melt-blowing in the previous section. As expected, η_s values of $(PLA_xFP_y)_{90}ATBC_{10}$ resins measured at varying shear rates are significantly lower than those of the PLA resin. In fact, η_s values of $(PLA_xFP_y)_{90}ATBC_{10}$ resins reduce only slightly as their FP contents increase, wherein the η_s values of $(PLA_xFP_y)_{90}ATBC_{10}$ resins with the increasing FP contents equal to or less than 5 wt % are indeed slightly higher than those of $PLA_{90}ATBC_{10}$ resin measured at varying shear rates. Regardless of the ATBC contents in FP_xATBC_y resins, η_s values of FP_xATBC_y resins measured at varying shear rates are less than

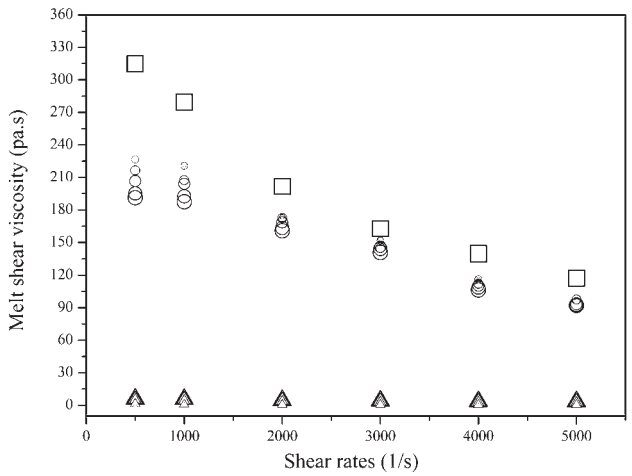

Figure 7 Melt shear viscosities of PLA (□), $PLA_{90}ATBC_{10}$ (○), $(PLA_{97.5}FP_{2.5})_{90}ATBC_{10}$ (○), $(PLA_{95}FP_5)_{90}ATBC_{10}$ (○), $(PLA_{92.5}FP_{7.5})_{90}ATBC_{10}$ (○), $(PLA_{90}FP_{10})_{90}ATBC_{10}$ (○), $(PLA_{85}FP_{15})_{90}ATBC_{10}$ (○), $(PLA_{80}FP_{20})_{90}ATBC_{10}$ (○), FP (Δ), $FP_{97.5}ATBC_{2.5}$ (Δ), $FP_{95}ATBC_5$ (Δ), $FP_{90}ATBC_{10}$(Δ), $FP_{85}ATBC_5$ (Δ) specimens measured at 190°C and varying shear rates.

6 pa s, which are significantly lower than those of PLA and $PLA_{90}FP_{10}$ resins. In which, η_s values of FP_xATBC_y resins measured at varying shear rates reduce only slightly as their FP contents increase.

Figure 8 exhibits the melt strength values of PLA_xFP_y blends measured at 170°C. It is interesting to note that melt strength values of PLA_xFP_y resins measured at 170°C increase with the increase in FP contents and reach a maximum value as the FP content approach 5 wt %, in which the maximum melt strength value of $PLA_{95}FP_5$ resin is about 2.3 time that of the virgin PLA resin. At FP contents higher than 5 wt %, melt strength values of PLA_xFP_y resins measured at 170°C reduce reversely with the further increase in FP contents. In fact, at FP contents equal to or higher than 10 wt %, melt strength values of PLA_xFP_y resins measured at 170°C reach an asymptote value, which is very close to the melt strength value of virgin PLA resin. The melt strength values of PLA_xFP_y resins at temperatures higher than 170°C and $(PLA_xFP_y)_aATBC_b$ resins even at 170°C are too low to determine. Nevertheless, FP dependence on melt strengths of melt-blownable $(PLA_xFP_y)_{90}ATBC_{10}$ resins are expected to present, although their melt strengths are too low to determine at 250°C. The broken filaments found on $(PLA_xFP_y)_{90}ATBC_{10}$ nonwoven specimens with FP contents higher than 5 wt % are likely attributed to the overdrawing of melt-blown fibers with relatively low melt strengths.

The melt strengths of reactive PLA blends were related[32] to the presence of long chain branches in the blends, in which long chain branches participate in forming intermolecular interactions in the melt during elongation and increase the resistance to deformation. The reaction between the carboxylic acid groups of PLA molecules and the hydroxyl groups of FP molecules during the melt-blending processes of PLA_xFP_y resins was evidenced by FTIR analysis. Presumably, the beneficial effect of FP contents on melt strengths of PLA_xFP_y resins with FP contents $\leqq$5 wt % is attributed to the formation of FP grafted PLA molecules during their melt-blending processes. In fact, as evidenced by morphological analysis, excessive amounts (>5 wt %) of FP droplets were found to phase-separate from PLA matrices and likely without reaction with PLA molecules. The phase-separated FP droplets are expected to improve the fluidity but reduce the melt strengths of PLA_xFP_y resins. As a consequence, the melt strength values of PLA_xFP_y resins reduce significantly as the FP contents are more than 5 wt %.

Weight and thickness analysis of melt-blown nonwovens

Figure 9 summarized the weights and thicknesses of $(PLA_xFP_y)_{90}ATBC_{10}$ nonwoven specimens prepared using varying conveying rates. The prepared nonwovens are classified as thin, medium, and thick nonwoven specimens, when they were prepared using a conveying rate of 6, 8, and 12 m/min, respectively. As expected, the weight and thickness values of $(PLA_xFP_y)_{90}ATBC_{10}$ nonwoven specimens with a fixed FP content reduce significantly as the conveying rates increase (see Fig. 9). The weights of $(PLA_xFP_y)_{90}ATBC_{10}$ nonwoven specimens prepared at the same conveying rate remain nearly the same as their FP contents increase from 0 to 20 wt %. Similarly, at a fixed conveying rate, their thicknesses remain nearly unchanged as the FP contents increase from 0 to 5 wt %. In contrast, the thicknesses of thin,

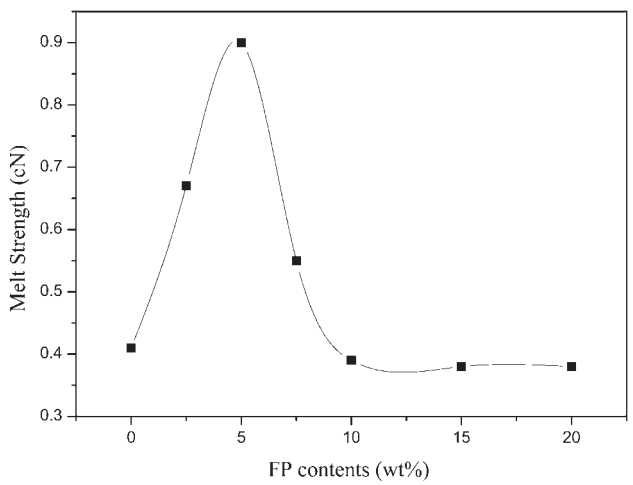

Figure 8 Melt strength values of PLA_xFP_y resins at 170°C.

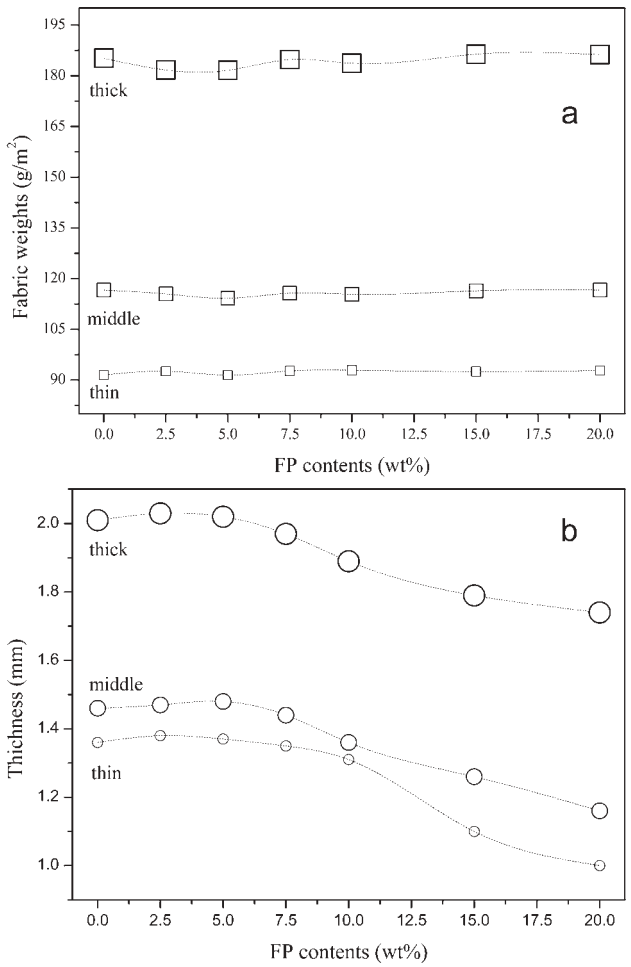

Figure 9 Fabric weight (□) and thickness (○) values of thin, middle and thick $(PLA_xFP_y)_{90}ATBC_{10}$ melt-blown nonwovens prepared at varying conveying rates.

medium and thick $(PLA_xFP_y)_{90}ATBC_{10}$ nonwoven specimens reduce significantly from 1.35, 1.44, and 1.97 mm to 1.31, 1.37, and 1.89 mm, respectively, as their FP contents increase from 7.5 to 10 wt %. As reported in morphological analysis, excessive amounts (>5 wt %) of FP droplets were found to phase-separate from PLA matrices. The phase-separated FP droplets are expected to improve the fluidity but reduce the melt strengths of PLA_xFP_y resins. The insufficient melt strengths of $(PLA_xFP_y)_{90}ATBC_{10}$ melts with relatively high FP contents are not expected to blow and form fluffy nonwovens but form poor melt-blown nonwovens with many melt-fractured blown fibers [see Fig. 5(e–g)]. The deleterious effect of FP content on thicknesses of $(PLA_xFP_y)_{90}ATBC_{10}$ nonwoven specimens with FP contents higher than 10 wt % is attributed to the reduction in melt strengths of $(PLA_xFP_y)_{90}ATBC_{10}$ resins with relatively high FP contents.

Tensile and bursting properties

The values of tensile and burst strengths of $(PLA_xFP_y)_{90}ATBC_{10}$ melt-blown specimens are summarized in Figures 10 and 11, respectively. The tensile and burst strengths of poorly formed $(PLA_xFP_y)_{90}ATBC_{10}$ melt-blown nonwovens with FP contents higher than 10 wt % are too low to determine. At a fixed nonwoven thickness, $PLA_{90}ATBC_{10}$ specimen exhibits relatively low tensile and burst strengths. After addition of FP in $(PLA_xFP_y)_{90}ATBC_{10}$ specimens, the tensile and burst strengths increase initially as the FP contents increase from 0 to 5 wt %. However, the tensile and burst strengths of the $(PLA_xFP_y)_{90}ATBC_{10}$ specimens reduce inversely as their FP contents increase from 5 to 10 wt %. As expected, the values of tensile and burst strengths of each $(PLA_xFP_y)_{90}ATBC_{10}$ melt-blown specimen improve significantly as their thicknesses increase.

As evidenced by morphological analysis, FP molecules appear to be compatible with PLA molecules

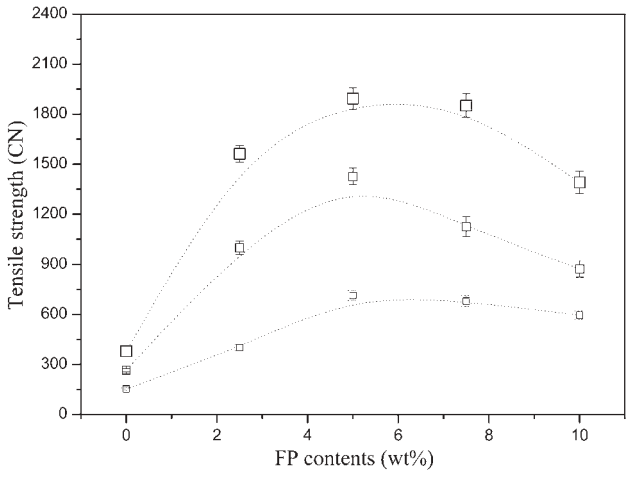

Figure 10 Tensile strength values of thin (□), middle (□) and thick (□) $(PLA_xFP_y)_{90}ATBC_{10}$ nonwovens.

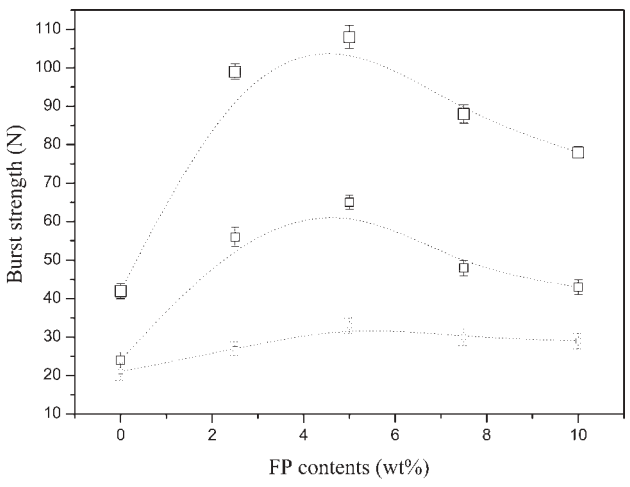

Figure 11 Burst strength values of thin (□), middle (□) and thick (□) $(PLA_xFP_y)_{90}ATBC_{10}$ nonwovens.

without clearly phase-separated FP phases, when FP contents are equal to or less than 5 wt %. However, at FP contents higher than about 5 wt %, distinct FP droplets were found phase-separating from PLA matrices. The poorly formed $(PLA_xFP_y)_{90}ATBC_{10}$ nonwoven specimens with FP contents equal to or higher than 5 wt % is likely attributed to the gradually appeared phase-separated FP droplets in the PLA matrices. By the same analogy, the reduction in tensile strength and burst strength values of $(PLA_xFP_y)_{90}ATBC_{10}$ specimens with further increasing FP contents are ascribed to the occurrence of phase-separated behavior between PLA and FP molecules and the poorly formed $(PLA_xFP_y)_{90}ATBC_{10}$ nonwoven fabrics as FP contents are higher than 5 wt %.

CONCLUSIONS

Rheological, melt strength, and melt-blown properties of $(PLA_xFP_y)_aATBC_b$ resins suggested that only $(PLA_xFP_y)_aATBC_{10}$ resins with proper rheological and melt strength properties are suitable for melt-blowing at a relatively high temperature at 250°C. The η_s values of $(PLA_xFP_y)_{90}ATBC_{10}$ resins reduce significantly and slightly as their ATBC and FP contents increase, respectively. The melt strength values of PLA_xFP_y resins measured at 170°C increase with the increase in FP contents and reach a maximum value as the FP content approach 5 wt %. As evidenced by SEM analysis, many FP droplets were found dispersing in the PLA matrix of the $(PLA_xFP_y)_{90}ATBC_{10}$ specimens, as their FP contents are more than 5 wt %. In contrast, FP molecules appear morphologically compatible with PLA molecules without distinct phase-separated FP droplets as FP contents equal to or less than 5 wt %. Further morphological analyses reveal that relatively fluffy and well formed nonwoven fabrics were found for $(PLA_xFP_y)_{90}ATBC_{10}$ nonwoven specimens melt-blown at FP contents equal to or lower than 5 wt %. In contrast, poor melt-blown characteristics with broken filaments gradually appear on $(PLA_xFP_y)_{90}ATBC_{10}$ nonwoven specimens as their FP contents increase. The initially significant reduction in T_g, T_{onset}, and T_m values of $(PLA_xFP_y)_{90}ATBC_{10}$ specimens with increasing FP contents is attributed to the compatible behavior between PLA and FP molecules. On the contrary, the increase in T_g, T_{onset}, and T_m values of $(PLA_xFP_y)_{90}ATBC_{10}$ specimens with further increasing FP contents is ascribed to the occurrence of phase-separated behavior between PLA and FP molecules at FP contents higher than 5 wt %, wherein the excess amounts of FP molecules not only invert but also bring additional FP molecules originally present in the PLA-rich phases into phase-separated FP droplets. In fact, addition of proper amounts of FP in $(PLA_xFP_y)_{90}ATBC_{10}$ resins can not only improve their melt-blown processibility but also effectively improve the tensile and burst strengths of their melt-blown nonwoven specimens.

References

1. Choi, K. J.; Spruiell, J. E.; Fellers, J. F. Polym Eng Sci 1988, 28, 81.
2. Lee, Y.; Wadsworth, L. C. Polym Eng Sci 1990, 30, 1413.
3. Bresee R. R. Int Nonwovens J 2004, 13, 49.
4. Wang, X. M.; Ke, Q. F. Polym Eng Sci 2006, 46, 1.
5. Zhang, D.; Sun Q. J Appl Polym Sci 2004, 94, 1218.
6. McCulloch, J. G. Int Nonwovens J 1999, 8, 139.
7. Sun, Q.; Zhang, D. J Appl Polym Sci 2004, 93, 2090.
8. Zhao, R.; Wadsworth, L. C. Polym Int 2003, 52, 133.
9. Muller, D. H.; Krobjilowski, A. Int Nonwovens J 2001, 10, 11
10. Wadsworth, L.; Sun, C.; Zhang, D. Nonwovens Industry 1999, 10, 1.
11. Zhao, R.; Wadsworth, L. C. Polym Int 2003, 52, 133.
12. Biresaw, G.; Carriere C. J. J Polym Sci B: Polym Phys 2002, 40, 2248.
13. Garlotta, D. J Polym Environ 2001, 9, 63.
14. Sinclair, R. G. Antec 1987, 237, 1214.
15. Kricheldorf, H. R.; Kreiser-Saunders, I. Macromol Symp 1996, 103, 85.
16. Eling, B.; Gogolewski, S.; Pennings, A. J. Polymer 1982, 23, 1587.
17. Fambri, L.; Pegoretti, A.; Fenner, R. Polymer 1997, 38, 79.
18. Leenslag, J. W.; Pennings, A. J. Polymer 1987, 28, 1602.
19. Horacek, I.; Kalisek, V. J Appl Polym Sci 1994, 54, 1759.
20. Tsuji, H.; Ikada, Y.; Hyon, S. H. J Appl Polym Sci 1994, 51, 337.
21. Kim, K.; Yu, M.; Zong, X. Biomaterials 2003, 24, 4977.
22. Zong, X.; Bien, H.; Chung, C. Y. ACS Polym Preprints 2003, 44, 96.
23. Qu, Y. H.; Ke Q. F. Proceedings of the Textile Institute 83rd World Conference, Shanghai, 2004, 1056.
24. Dever, M. India J. Nonwovens Res 1993, 5, 27.
25. Labrecque, L. V.; Kumar, R. A. J Appl Polym Sci 1997, 66, 1507.
26. Ljungberg, N.; Wesslen, B. J Appl Polym Sci 2002, 86, 1227.
27. Ljungberg, N.; Wesslen, B. J Appl Polym Sci 2003, 88, 3239.
28. Yeh, J. T.; Tsou, C. H.; Chai, W. L.; Wu, C. J.; Huang, C. Y.; Chen, K. N.; Wu, C. S. J Appl Polym Sci 2010, 116, 680.
29. Yeh, J. T.; Tsou, C. H.; Lu, W.; Li, Y. M.; Xiao, H. W.; Huang, C. Y.; Chen, K. N.; Wu, C. S.; Chai, W. L. J Polym Sci B: Polym Phys 2010, 48, 913.
30. Onteniente, J. P.; Abbes, B.; Safa, L. H. Starch/Starke 2000, 52, 112.
31. Wu, C. S. Polym Degrad Stab 2003, 80, 127.
32. Xu, Y. Q; Qu, J. P. J Appl Polym Sci 2009, 112, 3185.